Posttranscriptional Regulation of 14q32 microRNAs by RNA Binding Proteins CIRBP and HADHB during Vascular Regeneration after Ischemia

Accepted Manuscript

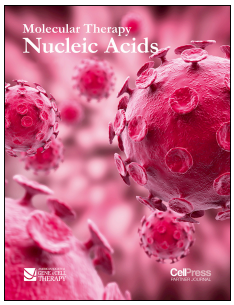

Posttranscriptional Regulation of 14q32 microRNAs by RNA Binding Proteins CIRBP and HADHB during Vascular Regeneration after Ischemia

Angela Downie Ruiz Velasco, Sabine M.J. Welten, Eveline A.C. Goossens, Paul H.A. Quax, Juri Rappsilber, Gracjan Michlewski, A.Yaël Nossent

PII: S2162-2531(18)30313-5

DOI: https://doi.org/10.1016/j.omtn.2018.11.017

Reference: OMTN 404

To appear in: *Molecular Therapy: Nucleic Acid*

Received Date: 7 September 2018

Accepted Date: 21 November 2018

Please cite this article as: Ruiz Velasco AD, Welten SMJ, Goossens EAC, Quax PHA, Rappsilber J, Michlewski G, Nossent AY, Posttranscriptional Regulation of 14q32 microRNAs by RNA Binding Proteins CIRBP and HADHB during Vascular Regeneration after Ischemia, *Molecular Therapy: Nucleic Acid* (2019), doi: https://doi.org/10.1016/j.omtn.2018.11.017.

Posttranscriptional Regulation of 14q32 microRNAs by RNA Binding Proteins CIRBP and HADHB during Vascular Regeneration after Ischemia

Angela Downie Ruiz Velasco[1,2*], Sabine M.J. Welten[3,4*], Eveline A.C. Goossens[3,4], Paul H.A. Quax[3,4], Juri Rappsilber[2,5], Gracjan Michlewski[1,2,6†], A. Yaël Nossent[3,4†]

[1]Division of Infection and Pathway Medicine, University of Edinburgh, The Chancellor's Building, Edinburgh, United Kingdom; [2]The Wellcome Centre for Cell Biology, University of Edinburgh, United Kingdom; [3]Department of Surgery; Leiden University Medical, The Netherlands; [4]Einthoven Laboratory for Experimental Vascular Medicine, Leiden University Medical, The Netherlands; [5]Department of Biotechnology, Technische Universität Berlin, Berlin, Germany; [6]Zhejiang University-University of Edinburgh Institute, Zhejiang University School of Medicine, Zhejiang University, Haining, Zhejiang, P.R. China

[*]These authors contributed equally
[†]These authors contributed equally

Correspondence should be addressed to G.M. (gracjan.michlewski@ed.ac.uk) and A.Y.N (a.y.nossent@lumc.nl)

Running Title: **Posttranscriptional regulation of 14q32 microRNAs**

Key words: microRNA, 14q32, ischemia, HADHB, CIRBP, hindlimb ischemia model

Abstract

After induction of ischemia in mice, 14q32 microRNAs are regulated in three distinct temporal patterns. These expression patterns, as well as basal expression levels, are independent of the miR genes' order in the 14q32 locus. This implies that posttranscriptional processing is a major determinant of 14q32 microRNA expression. Therefore, we hypothesized that RNA binding proteins (RBPs) regulate posttranscriptional processing of 14q32 and we aimed to identify these RBPs.

In order to identify proteins responsible for this posttranscriptional regulation we used RNA pull-down SILAC mass spectrometry (RP-SMS) on selected precursor microRNAs.

We observed differential binding of Cold Inducible RNA Binding Protein (CIRBP) and Hydroxyacyl-CoA Dehydrogenase Trifunctional Multienzyme Complex Subunit Beta (HADHB) to the precursors of late upregulated miR-329-3p and unaffected miR-495-3p. Immunohistochemical staining confirmed expression of both CIRBP and HADHB in the adductor muscle of mice. Expression of both CIRBP and HADHB was upregulated after hind limb ischemia in mice. Using RBP immunoprecipitation experiments, we showed specific binding of CIRBP to pre-miR-329, but not to pri-miR-329. Finally, using CRISPR/Cas9, we generated HADHB-/- 3T3 cells, which display reduced expression of miR-329 and miR-495, but not their precursors. These data suggest a novel role for CIRBP and HADHB in posttranscriptional regulation of 14q32 microRNAs.

Introduction

MicroRNAs (miRs) are short, non-coding RNA molecules (~22 nucleotides) that decrease expression of their target genes via translational repression[1]. MiR genes are transcribed by RNA polymerase II as primary miR (pri-miR) transcripts. Subsequently, the microprocessor complex, containing the RNase III Drosha and co-factor DGCR8, processes these pri-miRs into precursor miRs (pre-miRs) about 70 nucleotides long. Pre-miRs are exported to the cytoplasm where the enzyme Dicer cleaves the pre-miR into a miR duplex. Generally, one strand of the miR duplex (guide strand) is preferred for association with an Argonaute (AGO) protein and loading into the RNA induced silencing complex (RISC). However, accumulating evidence suggests that the other strand (passenger strand) can also be loaded into the RISC[2, 3]. MiRs guide the RISC to specific mRNA targets, in order to control mRNA translation[1]. A single miR is able to target numerous genes and by doing so, that miR can regulate complex, physiological processes. Over the past decade, miRs have been shown to play an important role in human disease, including cardiovascular disease[4-8]. Although miRs regulate physiological and pathological processes via modulation of target gene expression, miR expression itself is also subject to regulation.

MiR expression can be regulated at transcriptional as well as posttranscriptional level. Processing of miR precursors is controlled during the conversion of pri-miR to pre-miR through modulation of Drosha/DGCR8 activity[9-16]. The conversion of pre-miR to mature miR is regulated at the level of Dicer cleavage. RNA binding proteins (RBPs) have been found to bind sequences in the terminal loop and stem of pri-miRs, thereby enhancing or inhibiting pri- to pre-miR cleavage[9, 11, 16-18]. For example, processing of pri-miRs with conserved terminal loop regions, such as pri-miR-18a or pri-let-7a, have been shown to be stimulated and inhibited by hnRNP A1 protein, respectively[11, 12, 19]. In addition, p53 and SMADs have been reported to interact indirectly with Drosha and modulate pri- to pre-miR cleavage[9, 13]. The

RNA binding proteins LIN28a and LIN28b were reported to block accumulation of let-7 levels by repression of both Drosha[18, 20, 21] and Dicer[20, 22-25].

Many miRs are encoded within clusters and can be transcribed as long polycistronic transcripts. With 54 miR precursors, the 14q32 cluster is the largest polycistronic miR gene cluster in humans to our knowledge. In mice, this cluster is located on chromosome 12F1 and contains 61 miR genes. We have previously described the differential regulation of 14q32 miRs in a mouse model for ischemia in the hind limb[26]. Furthermore, we showed that 14q32 miR expression can be regulated by the transcription factor MEF2A, but not via altered transcription but via direct binding of MEF2A to precursor miRs[27]. The miRs from the 14q32 cluster follow three different expression patterns after induction of ischemia. Some miRs are upregulated early (early upregulated), some late (late upregulated) and the levels some miRs remain unchanged (unaffected). These patterns are independent of the chromosomal location of the 14q32 miR genes. Furthermore, baseline expression levels of these 14q32 miRs vary greatly. These findings indicate that individual 14q32 miR expression is regulated predominantly at posttranscriptional level[26].

We hypothesized that RNA binding proteins (RBPs) regulate posttranscriptional processing of 14q32 miRs and in this study we aimed to identify these RBPs. We could show that 14q32 miRs are indeed regulated at posttranscriptional level. We identified two RBPs (Cold Inducible RNA Binding Protein (CIRBP) and Hydroxyacyl-CoA Dehydrogenase Trifunctional Multienzyme Complex Subunit Beta (HADHB) that bind and aid in the processing of specific 14q32 miR precursors. This helps to explain the differential expression of 14q32 miRs under ischemia and expands our knowledge of regulation of miR biogenesis under pathological conditions. As 14q32 microRNAs play a crucial role in post-ischemic neovascularization, understanding how the 14q32 miRs are controlled will be relevant to future molecular therapies in cardiovascular disease.

Results

In vivo miR regulation

MiR microarray was performed in order to determine differential expression of miRs after induction of ischemia *in vivo*. MiRs from the 14q32 cluster showed three different temporal expression patterns after single ligation of the femoral artery. One third of the 14q32 miRs were upregulated within 24 hours after ischemia induction (early upregulated, Figure 1A, average expression Figure 1B). Another third of 14q32 miRs were upregulated 72 hours after induction of ischemia (late upregulated, Figure 1C, average expression Figure 1D), whereas the other 14q32 miRs were not differentially expressed after ischemia (unaffected, Figure 1E, average expression Figure 1F). When looking at the distribution of early and late upregulated and unaffected miRs on the 14q32 locus, there was no association between the expression profiles of miRs and their corresponding gene's chromosomal location (Figure 1G). In addition, baseline expression levels of 14q32 miRs were variable and also independent of their corresponding gene's chromosomal location. Because of their proven efficacy in post-ischemic neovascularization, we focused on early upregulated miR-494-3p, late upregulated miR-329-3p and unaffected miR-495-3p for further experiments[26].

Pri-miR, pre-miR and mature miR levels of 14q32 miRs

MiRs are transcribed as primary transcripts (pri-miRs), which are cleaved into precursor miRs (pre-miRs) inside the nucleus by DROSHA/DCGR8. The pre-miRs are then transported into the cytoplasm and cleaved further into mature miRs by DICER, potentially facilitated by other RBPs (Figure 2A). Using specific primers for each of the processing steps of three 14q32 miRs; miR-329-3p, miR-494 and miR-495-3p, we determined the expression levels of the pri-miR, pre-miR and mature miRs in the adductor muscle tissue after induction of

ischemia in mice. Expression of pri-miR-329 decreased slightly after induction of ischemia but increased in expression by day 7 after induction of ischemia. Pre-miR-329 followed expression of pri-miR-329 at 24 hours after ischemia but continued to decrease until 72 hours after ischemia induction. Expression of mature miR-329-3p showed an opposite trend to that of pre-miR-329 (Figure 2B). For early upregulated miR-494, expression of the pri-miR transcript was also decreased at 24 and 72 hours after ischemia induction. The abundance of pre-miR-494 however was only slightly reduced 24 hours after ischemia, whereas mature miR-494-3p levels were upregulated (Figure 2C). Expression of pri-miR-495 and pre-miR-495 followed the same pattern after ischemia, showing decreased expression within 24 hours, which continued at later time points (Figure 2D). Despite this, mature miR-495-3p levels remained unchanged after ischemia induction. In general, whereas pre-miR expression levels declined, we observed increased (miR-494, miR-329) or sustained (miR-495) expression of mature miR levels. This suggests that regulation of 14q32 miR-329, miR-494 and miR-495 processing takes place at the conversion of pre-miR to mature miR.

Pre-miR pull down followed by SILAC Mass Spectrometry reveals putative 14q32 miR biogenesis factors

We decided to further explore this regulation by comparing the pre-miR interacting protein partners of the upregulated miR-329 and the unaffected miR-495, upon serum-starvation in 3T3 cells, mimicking the nutrient depravation during ischemia. We did not pursue miR-494 due to lack of response in our *in vitro* starvation model. To identify the RBPs responsible for differential expression of these two miRs via posttranscriptional regulation, we performed RNA-pulldown Stable Isotope Labelling of Amino Acids (SILAC) mass spectrometry (RP-SMS) (Figure 3A-B). We identified a number of proteins, which were specifically bound to

pre-miR-329 and pre-miR-495, namely RBM28 and TBL3 (pre-miR-329 specific), RBM15 (pre-miR-495 specific) as well as proteins CKAP4, P4HB, CIRBP and HADHB, which were bound to both pre-miR-329 and pre-miR-495, showing an increase in binding after serum starvation. Using Western Blot analysis, we could only validate binding of HADHB and CIRBP to miR-329 and miR-495 precursors (Figure 3C-F). This could either be due the quality of the available antibodies against other identified proteins or due to low expression levels. While both HADHB and CIRBP showed a general increase in binding upon serum starvation to both pre-miRs, this was particularly evident in the case of HADHB binding to pre-miR-329, which displayed little to no binding in non-starvation conditions but showed an increase in binding upon starvation. A more modest increase in HADHB binding to pre-miR-495 was also observed, where in contrast to pre-miR-329, this protein also binds in normal serum conditions.

CIRBP and HADHB expression in vivo

We next determined expression of RNA binding proteins CIRBP and HADHB *in vivo* in the adductor muscle at different timepoints after induction of ischemia. Using immunohistochemistry, expression of both CIRBP and HADHB was confirmed in the adductor muscle of mice on day 1 after ischemia. Expression of CIRBP and HADHB was dispersed throughout the cells (Figure 4A and 4B, respectively). At mRNA level, expression of CIRBP was increased within 24 hours after induction of ischemia, whereas HADHB mRNA was increased at 3 days after induction of ischemia (Figures 4C and 4D). Importantly, this timepoint (day 3) corresponds to the maximum changes observed for levels of mature miR-329, as well as pre-miR-329 and pre-miR-495 after induction of ischemia. Next, we wanted to confirm a change in protein expression using western blot. Due to low signal,

CIRBP protein levels could not be detected. Importantly however, we were able to confirm an increase of HADHB in the adductor muscle at day 3 after induction of ischemia compared to day 0 and day 1 (Figure 4E), in line with the results obtained for HADHB mRNA.

HADHB and CIRBP binding to miR-329 pri-miR, pre-miR and mature miR transcripts

To determine interaction between HADHB and CIRBP and 14q32 miR-329 and miR-495 precursors, RNA immunoprecipitation (RIP) experiments were performed using antibodies against these RBPs or a negative control IgG in 3T3 cell cultures. Whereas HADHB was shown to bind to both pri-miR-329 and pre-miR-329, CIRBP showed specific binding to pre-miR-329, not to pri-miR-329 (Figure 5). CIRBP and HADHB both bind the mature miR-329-3p. Expression of pri-miR-495 and pre-miR-495 was too low to either confirm or exclude binding of CIRBP or HADHB. RIP experiments using an unrelated RBP that has been shown to regulate processing of polycistronic miRs, namely SND1[28], showed no specific binding to either pri-miRs or pre-miRs of miR-329 and miR-495 (Supplemental Figure 1).

Changes in miR levels in CRISPR/Cas9 generated HADHB KO cell lines

Next, we sought to understand the effects that depletion of CIRBP and HADHB would have on the levels of miR-329 and miR-495. To achieve this, we used CRISPR/Cas9 to generate 3T3 KO cell lines. Our attempts to generate a CIRBP KO line were unsuccessful. This indicates that the protein could be essential for 3T3 cell vitality. Nevertheless, we identified two colonies (AQ and Z) grown from individual cells that had been targeted for disruption of HADHB. These colonies showed complete depletion of HADHB as measured by western blot (Figure 6A). We confirmed this deletion by sequencing the region surrounding the targeted

sequence (Figure 6B). All the sequences identified either correspond to a frame-shift deletion, or a deletion spanning an exon-intron junction.

Following this, we analysed the levels of mature miR-329 and miR-495 by qRT-PCR, in colony AQ. We observed a decrease of over 80% in the levels of both mature miR-329-3p and miR-495-3p (Figure 6D). Importantly, the expression of miR-423, a widely expressed and stable miR, not from the 14q32 cluster, did not change (Figure 6D). This suggests that the downregulation of mature miR-329-3p and miR-495-3p in HADHB knockout cells is specific and not due to a global reduction in mature miR levels. Finally, we determined the levels of the pre-miR-329 and pre-miR-495 and showed lack of statistically significant change (Figure 6E). Similar results were obtained for colony Z (data not shown). This corroborates our *in vivo* results as well as showing that HADHB is involved in post-transcriptional regulation of miRs from the 14q32 cluster at the level of pre-miR to mature miR cleavage.

Discussion

In this study, we investigated posttranscriptional regulation of 14q32 miRs during ischemia. Using specific primers for each of the miR processing steps, we found that increased expression of 14q32 miRs after hind limb ischemia is not determined by increased transcription, but that it is the result of increased processing of pre-miR to miR. We have used serum starvation of 3T3 cells to mimic certain aspects of hind limb ischemia. This allowed us to investigate which RBPs can bind to pre-miR transcripts of 14q32 miRs. Using RNA pull-down and quantitative mass spectrometry (RP-SMS) we have found that CIRBP and HADHB bind to miR-329 and miR-495 precursors. We confirmed expression and upregulation of these RBPs in murine muscle tissues during ischemia, at mRNA level as well as protein level for HADHB. Furthermore, we have shown that upon deletion of HADHB from 3T3 cells by CRISPR/Cas9, levels of mature miR-329-3p and miR-495-3p, but not pre-miR-329 or pre-miR-495, are significantly reduced. These data are consistent with our *in vivo* data, supporting the hypothesis that HADHB is involved in the post-transcriptional regulation of these miRs in the pre-miR to mature miR processing step. Further in-depth analysis will be necessary to uncover the mechanism and physiological significance of HADHB- (and CIRBP-) mediated regulation of microRNA biogenesis.

Posttranscriptional regulation of polycistronic miRs has been described previously. In fact, differential expression after induction of hindlimb ischemia, similar to that of the 14q32 miRs, has also been shown for miRs of the polycistronic miR-17-92a cluster. The miR-17-92a cluster encodes for seven miRs and is transcribed as one single primary transcript[29]. However, individual members of the miR-17-92a cluster were differentially expressed during endothelial differentiation of murine embryonic stem cells[30]. The SND1 protein, which is a component of the RISC, was found to bind to pri-miRs, pre-miRs and mature miRs of the miR-17-92a cluster. Silencing of SND1 reduced processing of miR-17-92a cluster members,

especially under hypoxic conditions[28]. Here, we could not demonstrate binding of SND1 to either pri-miRs or pre-miRs of 14q32 miRs miR-329 and miR-495 using RIP experiments. Our data demonstrated that processing of 14q32 miRs miR-329 and miR-495 is independent of SND1 binding, but instead relies on CIRBP and HADHB.

CIRBP is an evolutionary conserved RBP that is transcriptionally upregulated in low temperature conditions or other conditions of stress, including ischemia[31, 32]. CIRBP protein is predominantly expressed in the nucleus, but can also be transported to the cytoplasm under physiological or stressful conditions[33]. In our immunohistochemical stainings (Figures 4A and 4B), CIRBP, and HADHB, were observed in both the nucleus and the cytoplasm of intramuscular arteriolar wall cells. MiR processing from pre-miR to mature miR also occurs in the cytoplasm. CIRBP is involved in posttranscriptional regulation of mRNAs[34]. Here however, we showed for the first time that CIRBP could be involved in posttranscriptional regulation of miRs. Future experiments will have to determine whether CIRBP can also regulate other miRs during ischemia.

HADHB forms the beta subunit of the mitochondrial trifunctional protein, which catalyzes the last steps of mitochondrial beta-oxidation of long chain fatty acids. In addition, HADHB was found to act as an RBP and bind renin mRNA, leading to its destabilization[35]. Localization of HADHB was found to be predominantly in mitochondria, but also in the cytoplasm and nucleoli of Calu-6 cells[36]. In this study, we observed both cytoplasmic as well as nuclear expression of both HADHB and CIRBP in murine adductor muscle tissue after ischemia. In addition, we have now shown that HADHB can also bind pri-miRs, pre-miRs and mature miRs of the 14q32 miR cluster, indicating its role in posttranscriptional regulation of miR expression under ischemia.

Regulation of miR processing under stress conditions, such as hypoxia, has been previously reported by several studies[37-39]. In endothelial cells, hypoxia was shown to both increase expression of certain miRs (such as miR-210[39]) as well as to reduce miR processing[38]. Further examination revealed that chronic hypoxia down-regulated expression of Dicer, reducing subsequent miR processing[38]. More recently, the involvement of the Epidermal Growth Factor Receptor (EGFR) in miR processing under hypoxic conditions was reported. EGFR was shown to increase phosphorylation of AGO2 under hypoxic conditions, which reduced AGO2 binding to Dicer and subsequent miR processing from pre-miR to mature miR by Dicer[26, 40, 41]. Although we did not study regulation of 14q32 miR processing under true hypoxic conditions *in vitro*, we were able to demonstrate increased binding of CIRBP and HADHB to pre-miRs under conditions of serum starvation, which is a major contributor of cellular stress after artery occlusion *in vivo*.

In this study, we identified RBPs that bind and regulate specific 14q32 miR precursors. These results provide insights into the complex regulation of the 14q32 miRs. We showed for the first time that CIRBP and HADHB, which have been shown to control posttranscriptional regulation of mRNAs, could also be involved in posttranscriptional processing of miRs. Finally, we demonstrated that depletion of HADHB in 3T3 cells has a negative effect on selected 14q32 miR expression levels. Through manipulation of CIRBP and HADHB, which control expression of 14q32 miRs, we may be able to influence 14q32 miR expression higher up the regulatory cascade, potentially having more profound therapeutic effects on post-ischemic neovascularization. As ischemic cardiovascular disease is still one of the leading causes of death worldwide, novel therapeutic options to induce neovascularization remain highly needed.

Materials and Methods

Hind limb ischemia model

All experiments were approved by the committee on animal welfare of the Leiden University Medical Center (Leiden, the Netherlands. Approval reference numbers 09163 and 10243). This study was conducted in accordance with the Dutch government guidelines and the Directive 2010/63/EU of the European Parliament. Unilateral hind limb ischemia was induced in healthy adult male C57BL6 mice by single ligation of the left femoral artery, as previously described[26, 41]. Briefly, electrocoagulation of the femoral artery was performed proximal to the superficial epigastric artery. C57Bl/6 mice (n=4 per timepoint) were sacrificed at several timepoints (day 0 (before ligation of the femoral artery), day 1, 3, 7, 10, 14 and 28) after hind limb ischemia induction[42, 43]. Upon sacrifice, the adductor muscles were harvested and either snap-frozen on dry ice or fixed in 4% paraformaldehyde.

Microarray

For microarray analysis, total RNA was isolated from adductor muscles using the RNeasy fibrous tissue minikit (Qiagen). RNA concentration, purity and integrity were analysed by nanodrop (Nanodrop® Technologies) and Bioanalyzer (Agilent 2000) measurements. Animals

For miR expression profiling, adductor muscle tissue of day 0, 1, 3 and 7 after induction of hind limb ischemia was used. MiR expression profiling was performed as previously described, using LNA based arrays (miRCURY LNA™ miR Array ready-to-spot probe set, Exiqon)[26]. Normalization and background correction were performed in the "statistical language R" using "vsn" package (Bioconductor). Differential expression was assayed using the "limma" package (Bioconductor) by fitting the eBayes linear model and contrasting

individual treatments with untreated controls. Log2 fold changes were calculated using the toptable function of the limma package[4, 44].

For whole genome expression profiling, adductor muscle tissue of day 0, 1, 3, 7, 14 and 28 after induction of hind limb ischemia was used. Whole genome expression profiling was performed using MouseWG-6 v2.0 Expression Beadchips (Illumina) and expression levels were Log2-transformed, as previously described[26, 42].

Cell culture

3T3 cells were cultured at 37ºC in a humidified 5% CO_2 environment. Culture medium consisted of DMEM GlutaMAX™ (Gibco) supplemented with 10% heat inactivated fetal calf serum (PAA) and 1% penicillin/streptomycin (PAA). Culture medium was refreshed every 2-3 days. Cells were passed using trypsin-EDTA (Sigma) at 90% confluency.

In vitro cellular starvation model

To mimic the effects of nutrient depravation after *in vivo* ischemia, 3T3 cells were cultured under serum starvation conditions (DMEM glutaMAX™ supplemented with 0.5% heat inactivated fetal calf serum and 1% penicillin/streptomycin). Cells were starved for 24 hours under serum starved conditions after which they were collected and processed as necessary.

RNA pull-down and SILAC Mass Spectrometry (RP-SMS)

RNA pull-down and mass spectrometry were performed as described previously, with slight modifications. In brief, total protein extracts from normal serum and serum starved 3T3 cells grown in 'light' [^{12}C]Arg/[12C]Lys and 'heavy' [^{13}C]Arg/[^{13}C]Lys isotopes, respectively, were incubated with in vitro transcribed RNAs chemically coupled to agarose beads. The incubation was followed by a series of washes with buffer G (20 mM Tris pH 7.5, 135 mM

NaCl, 1.5 mM MgCl2, 10% (v/v) glycerol, 1 mM EDTA, 1 mM DTT and 0.2 mM PMSF). After the final wash, the proteins associated with the RNA on the beads were analyzed by SDS–PAGE followed by in-gel digestion and mass spectrometry or western blotting.

Western Blot Analysis

Total protein samples from 3T3 cells (100 μg per lane), isolated by sonication, were resolved by standard NuPAGE SDS–PAGE electrophoresis with MOPS running buffer (Life Technologies) and transferred onto a nitrocellulose membrane. Total protein samples from murine adductor muscle tissue were isolated using a standard TRIzol protocol (Thermo Fisher) at day 0, 1, and 3 after induction of ischemia. The membrane was blocked overnight at 4°C with 1:10 western blocking reagent (Roche) in TBS buffer with 0.1% Tween-20 (TBST). The following day, the membrane was incubated for 1 h at room temperature with primary antibody solution in 1:20 western blocking reagent diluted in TBST in the following concentrations; rabbit polyclonal CIRBP (Protein Tech 10209-2-AP) 1:1000, rabbit polyclonal HADHB (LSBio-LS-C334236) 1:2500. After washing in TBST, the blots were incubated with the appropriate secondary antibody conjugated to horseradish peroxidase and detected with SuperSignal West Pico detection reagent (Thermo Scientific). The membranes were stripped using ReBlot Plus Strong Antibody Stripping Solution (Chemicon) equilibrated in water, blocked in 1:10 western blocking solution in TBST and re-probed as described above. Western Blots were quantified using ImageJ analysis software (1.48v, NIH) and ImageStudio (Licor) and normalized to the input.

RNA immunoprecipitation

RNA immunoprecipitation (RIP) was performed using the EZMagna RIP kit (Millipore), according to manufacturer's instructions. 3T3 cells were grown to 90% confluency and lysed

in complete RIP lysis buffer. Cell lysates were incubated with RIP buffer containing magnetic beads conjugated with antibodies against Cold Induced RNA binding protein (CIRBP, Abcam ab106230), hydroxyacyl-CoA dehydrogenase/3-ketoacyl-CoA thiolase/enoyl-CoA hydratase (trifunctional protein), beta subunit (HADHB, Novus Biologicals NBP1-82609), SND1 (Abcam ab71186) and rabbit control IgG (Millipore PP64B). Before immunoprecipition, 10% of cell lysate was taken and served as input control. Next, samples were treated with proteinase K to digest protein and RNA was isolated using a standard TRIzol-chloroform extraction protocol.

RT/qPCR

Adductor muscles from day 0 and day 1, 3 and 7 after surgery were homogenized by grounding with a pestle and mortar in liquid nitrogen. Total RNA was isolated using a standard TRIzol-chloroform extraction protocol. RNA concentration and purity were determined by nanodrop (Nanodrop® Technologies). RNA was reverse transcribed using high-capacity RNA to cDNA RT kits (Life Technologies, USA). Relative quantitative mRNA PCR was performed on reverse transcribed cDNA using, SYBR® green dye (Qiagen). Primers for pri-miRs, pre-miRs, HADHB and CIRBP were designed using Primer3. Sequences of primers are listed in Supplementary Table 1. MiR quantification was performed using Taqman® miR assays (Applied Biosystems) according to manufacturer's protocol. Relative quantitative PCR was performed on the Viia7 system (Applied Biosystems) and amplification efficiencies were checked by standard curves. Data were normalized using a stably expressed endogenous control (snRNA-U6).

Levels of mature miRs in 3T3 WT and HADHB KO cells were measured using miRScript RT (Qiagen) and SYBR® green (Qiagen). The levels of pre-miRs were also measured by

miRScript RT (Qiagen) and SYBR® green (Qiagen) with prior fractionation of total RNA on 10% denaturing polyacrylamide gel to isolate the fraction containing RNAs from 50nt to 100nt. MiR and pre-miR levels were normalized to miR-16 and pre-miR-16, as both proved highly stable in 3T3 cells.

Immunohistochemical staining

Formaldehyde fixed adductor muscles were paraffin-embedded and 5 µm thick cross-sections of muscles were stained to visualize expression of RNA binding proteins. Cross sections of adductor muscles were re-hydrated and endogenous peroxidase activity was blocked. Antigen retrieval was performed with Citrate buffer (pH 6.0) at 100ºC for 10 minutes. Muscles were stained with rabbit polyclonal anti-HADHB (Novus Biologicals, NBP1-82609, 1:1000) or goat polyclonal anti-CIRBP (Abcam, ab106230, 1:400) to visualize HADHB and CIRBP respectively, and counterstained using haematoxylin.

Generation of HADHB KO by CRISPR/Cas9

3T3 cells were transfected with Cas9 containing-plasmid px458, which included guide RNAs targeting the third exon of HADHB as well as a GFP cassette to be used as a reporter for positive transfection. Single cell FACS sorting was carried out for selection of individual transfected cells which were then grown into colonies, from which genomic DNA was extracted. The region surrounding the Cas9 target was amplified by PCR and cloned into pJET cloning vector (Thermo K1232) and sequenced using pJET sequencing primers. Western Blot was then used to confirm protein level depletion for colonies showing deletions in this region.

Statistical Analyses

Analyses of the microRNA and mRNA microArrays is describe above.

Western blot and rt/qPCR data are represented as mean values ± SEM. Differences between groups were evaluated using one-way ANOVA followed by two-sample t-test (Figures 3 and 4) or one-sample t-test (Figure 6). P-values > 0.05 were considered statistically significant. The number of replicates is given in the figure legends.

Author contributions

Conceptualization – G.M and A.Y.N; Methodology – J.R., G.M and A.Y.N; Investigation – A.D.R.V., S.M.J.W, E.A.C.G; Writing – Original Draft - A.D.R.V., S.M.J.W, G.M and A.Y.N; Writing – Review & Editing - A.D.R.V., S.M.J.W, P.H.A.Q., G.M and A.Y.N,; Funding Acquisition J.R., G.M P.H.A.Q. and A.Y.N; Supervision- P.H.A.Q., G.M and A.Y.N.

Conflict of Interest

None.

Acknowledgements

We thank Christos Spanos for help with mass spectrometry.

Funding sources

A.D.R.V – CONACYT scholarship number 684300, and Prinicipal Carreer Development Scholarship (Edinburgh), J.R. - Wellcome Trust Senior Research Fellowship (084229), G.M - Medical Research Council Career Development Award (G10000564), Wellcome Trust Seed Award (210144/Z/18/Z) Wellcome Trust Centre Core Grants (077707 and 092076), A.Y.N – Netherlands Heart Foundation Dr. Dekker Senior Postdoc Grant (NHS-2014T102), S.M.J.W and P.H.A.Q – NIRM (FES0908).

References

1. Bartel, DP (2004). MicroRNAs: genomics, biogenesis, mechanism, and function. *Cell* **116**: 281-297.
2. Schober, A, Nazari-Jahantigh, M, Wei, Y, Bidzhekov, K, Gremse, F, Grommes, J, *et al.* (2014). MicroRNA-126-5p promotes endothelial proliferation and limits atherosclerosis by suppressing Dlk1. *Nature medicine* **20**: 368-376.
3. Yang, X, Du, WW, Li, H, Liu, F, Khorshidi, A, Rutnam, ZJ, *et al.* (2013). Both mature miR-17-5p and passenger strand miR-17-3p target TIMP3 and induce prostate tumor growth and invasion. *Nucleic acids research* **41**: 9688-9704.
4. Lu, M, Zhang, Q, Deng, M, Miao, J, Guo, Y, Gao, W, *et al.* (2008). An analysis of human microRNA and disease associations. *PloS one* **3**: e3420.
5. Lujambio, A, and Lowe, SW (2012). The microcosmos of cancer. *Nature* **482**: 347-355.
6. Im, HI, and Kenny, PJ (2012). MicroRNAs in neuronal function and dysfunction. *Trends in neurosciences* **35**: 325-334.
7. Ono, K, Kuwabara, Y, and Han, J (2011). MicroRNAs and cardiovascular diseases. *The FEBS journal* **278**: 1619-1633.
8. Welten, SM, Goossens, EA, Quax, PH, and Nossent, AY (2016). The multifactorial nature of microRNAs in vascular remodelling. *Cardiovasc Res* **110**: 6-22.
9. Suzuki, HI, Yamagata, K, Sugimoto, K, Iwamoto, T, Kato, S, and Miyazono, K (2009). Modulation of microRNA processing by p53. *Nature* **460**: 529-533.
10. Choudhury, NR, de Lima Alves, F, de Andres-Aguayo, L, Graf, T, Caceres, JF, Rappsilber, J, *et al.* (2013). Tissue-specific control of brain-enriched miR-7 biogenesis. *Genes & development* **27**: 24-38.
11. Michlewski, G, Guil, S, Semple, CA, and Caceres, JF (2008). Posttranscriptional regulation of miRNAs harboring conserved terminal loops. *Molecular cell* **32**: 383-393.
12. Guil, S, and Caceres, JF (2007). The multifunctional RNA-binding protein hnRNP A1 is required for processing of miR-18a. *Nature structural & molecular biology* **14**: 591-596.
13. Davis, BN, Hilyard, AC, Lagna, G, and Hata, A (2008). SMAD proteins control DROSHA-mediated microRNA maturation. *Nature* **454**: 56-61.
14. Sakamoto, S, Aoki, K, Higuchi, T, Todaka, H, Morisawa, K, Tamaki, N, *et al.* (2009). The NF90-NF45 complex functions as a negative regulator in the microRNA processing pathway. *Molecular and cellular biology* **29**: 3754-3769.
15. Wu, H, Sun, S, Tu, K, Gao, Y, Xie, B, Krainer, AR, *et al.* (2010). A splicing-independent function of SF2/ASF in microRNA processing. *Molecular cell* **38**: 67-77.
16. Trabucchi, M, Briata, P, Garcia-Mayoral, M, Haase, AD, Filipowicz, W, Ramos, A, *et al.* (2009). The RNA-binding protein KSRP promotes the biogenesis of a subset of microRNAs. *Nature* **459**: 1010-1014.
17. Michlewski, G, and Caceres, JF (2018). Post-transcriptional control of miRNA biogenesis. *RNA (New York, NY)*.
18. Viswanathan, SR, Daley, GQ, and Gregory, RI (2008). Selective blockade of microRNA processing by Lin28. *Science (New York, NY)* **320**: 97-100.
19. Michlewski, G, and Caceres, JF (2010). Antagonistic role of hnRNP A1 and KSRP in the regulation of let-7a biogenesis. *Nature structural & molecular biology* **17**: 1011-1018.

20. Newman, MA, Thomson, JM, and Hammond, SM (2008). Lin-28 interaction with the Let-7 precursor loop mediates regulated microRNA processing. *RNA (New York, NY)* **14**: 1539-1549.
21. Piskounova, E, Polytarchou, C, Thornton, JE, LaPierre, RJ, Pothoulakis, C, Hagan, JP, *et al.* (2011). Lin28A and Lin28B inhibit let-7 microRNA biogenesis by distinct mechanisms. *Cell* **147**: 1066-1079.
22. Choudhury, NR, Nowak, JS, Zuo, J, Rappsilber, J, Spoel, SH, and Michlewski, G (2014). Trim25 Is an RNA-Specific Activator of Lin28a/TuT4-Mediated Uridylation. *Cell reports* **9**: 1265-1272.
23. Heo, I, Joo, C, Kim, YK, Ha, M, Yoon, MJ, Cho, J, *et al.* (2009). TUT4 in concert with Lin28 suppresses microRNA biogenesis through pre-microRNA uridylation. *Cell* **138**: 696-708.
24. Heo, I, Joo, C, Cho, J, Ha, M, Han, J, and Kim, VN (2008). Lin28 mediates the terminal uridylation of let-7 precursor MicroRNA. *Molecular cell* **32**: 276-284.
25. Rybak, A, Fuchs, H, Smirnova, L, Brandt, C, Pohl, EE, Nitsch, R, *et al.* (2008). A feedback loop comprising lin-28 and let-7 controls pre-let-7 maturation during neural stem-cell commitment. *Nature cell biology* **10**: 987-993.
26. Welten, SM, Bastiaansen, AJ, de, JR, de Vries, MR, Peters, EH, Boonstra, M, *et al.* (2014). Inhibition of 14q32 MicroRNAs miR-329, miR-487b, miR-494 and miR-495 Increases Neovascularization and Blood Flow Recovery after Ischemia. *Circ Res*.
27. Welten, SMJ, de Vries, MR, Peters, EAB, Agrawal, S, Quax, PHA, and Nossent, AY (2017). Inhibition of Mef2a Enhances Neovascularization via Post-transcriptional Regulation of 14q32 MicroRNAs miR-329 and miR-494. *Mol Ther Nucleic Acids* **7**: 61-70.
28. Heinrich, EM, Wagner, J, Kruger, M, John, D, Uchida, S, Weigand, JE, *et al.* (2013). Regulation of miR-17-92a cluster processing by the microRNA binding protein SND1. *FEBS Lett* **587**: 2405-2411.
29. He, L, Thomson, JM, Hemann, MT, Hernando-Monge, E, Mu, D, Goodson, S, *et al.* (2005). A microRNA polycistron as a potential human oncogene. *Nature* **435**: 828-833.
30. Treguer, K, Heinrich, EM, Ohtani, K, Bonauer, A, and Dimmeler, S (2012). Role of the microRNA-17-92 cluster in the endothelial differentiation of stem cells. *Journal of vascular research* **49**: 447-460.
31. Wellmann, S, Buhrer, C, Moderegger, E, Zelmer, A, Kirschner, R, Koehne, P, *et al.* (2004). Oxygen-regulated expression of the RNA-binding proteins RBM3 and CIRP by a HIF-1-independent mechanism. *Journal of cell science* **117**: 1785-1794.
32. Jackson, TC, Manole, MD, Kotermanski, SE, Jackson, EK, Clark, RS, and Kochanek, PM (2015). Cold stress protein RBM3 responds to temperature change in an ultra-sensitive manner in young neurons. *Neuroscience* **305**: 268-278.
33. Zhu, X, Buhrer, C, and Wellmann, S (2016). Cold-inducible proteins CIRP and RBM3, a unique couple with activities far beyond the cold. *Cellular and molecular life sciences : CMLS* **73**: 3839-3859.
34. Lleonart, ME (2010). A new generation of proto-oncogenes: cold-inducible RNA binding proteins. *Biochimica et biophysica acta* **1805**: 43-52.
35. Adams, DJ, Beveridge, DJ, van der Weyden, L, Mangs, H, Leedman, PJ, and Morris, BJ (2003). HADHB, HuR, and CP1 bind to the distal 3'-untranslated region of human renin mRNA and differentially modulate renin expression. *The Journal of biological chemistry* **278**: 44894-44903.

36. Morris, BJ, Adams, DJ, Beveridge, DJ, van der Weyden, L, Mangs, H, and Leedman, PJ (2004). cAMP controls human renin mRNA stability via specific RNA-binding proteins. *Acta physiologica Scandinavica* **181**: 369-373.
37. Leung, AK, and Sharp, PA (2010). MicroRNA functions in stress responses. *Molecular cell* **40**: 205-215.
38. Ho, JJ, Metcalf, JL, Yan, MS, Turgeon, PJ, Wang, JJ, Chalsev, M, *et al.* (2012). Functional importance of Dicer protein in the adaptive cellular response to hypoxia. *The Journal of biological chemistry* **287**: 29003-29020.
39. Fasanaro, P, D'Alessandra, Y, Di Stefano, V, Melchionna, R, Romani, S, Pompilio, G, *et al.* (2008). MicroRNA-210 modulates endothelial cell response to hypoxia and inhibits the receptor tyrosine kinase ligand Ephrin-A3. *The Journal of biological chemistry* **283**: 15878-15883.
40. Shen, J, Xia, W, Khotskaya, YB, Huo, L, Nakanishi, K, Lim, SO, *et al.* (2013). EGFR modulates microRNA maturation in response to hypoxia through phosphorylation of AGO2. *Nature* **497**: 383-387.
41. Nowak-Sliwinska, P, Alitalo, K, Allen, E, Anisimov, A, Aplin, AC, Auerbach, R, *et al.* (2018). Consensus guidelines for the use and interpretation of angiogenesis assays. *Angiogenesis*.
42. Nossent, AY, Bastiaansen, AJ, Peters, EA, de Vries, MR, Aref, Z, Welten, SM, *et al.* (2017). CCR7-CCL19/CCL21 Axis is Essential for Effective Arteriogenesis in a Murine Model of Hindlimb Ischemia. *J Am Heart Assoc* **6**.
43. Simons, KH, Aref, Z, Peters, HAB, Welten, SP, Nossent, AY, Jukema, JW, *et al.* (2018). The role of CD27-CD70-mediated T cell co-stimulation in vasculogenesis, arteriogenesis and angiogenesis. *International journal of cardiology* **260**: 184-190.
44. van der Kwast, RV, van Ingen, E, Parma, L, Peters, HA, Quax, PH, and Nossent, AY (2017). A-To-I Editing of Microrna-487b Alters Target Gene Selection After Ischemia and Promotes Neovascularization. *Circulation research*.

Figure Legends

Figure 1. Differential expression patterns of 14q32 microRNAs after induction of ischemia. MiR expression was evaluated before induction of ischemia (T0) and day 1 (T1), day 3 (T3) and day 7 (T7) after induction of ischemia in whole adductor muscle of 4 mice per timepoint. (A) Early upregulated 14q32 miRs were upregulated within 24 hours after ischemia. (B) Average intensity of all early upregulated miRs. (C) Late upregulated 14q32 miRs were not upregulated until 72 hours after ischemia induction. (D) Average intensity of all late upregulated miRs. (E) Unaffected 14q32 miRs were not regulated after ischemia. (F) Average intensity of all unaffected miRs. (G) Chromosomal location of early upregulated (red), late upregulated (green) and unaffected (blue) miRs on the murine 12F1 locus.

Figure 2. MicroRNA Processing. (A) MiRs are transcribed as primary transcripts (pri-miRs), which are cleaved into precursor miRs (pre-miRs) inside the nucleus by DROSHA/DCGR8. The pre-miRs are then transported into the cytoplasm and cleaved further into mature miRs by DICER, potentially facilitated by unknown regulatory factors. (B-D) Pri-miR, pre-miR and mature miR expression levels of 14q32 miRs, measured in whole adductor muscle of 4 mice per timepoint. Percentage of expression (Relative to Day 0) at day 0 (no ischemia), day 1, day 3 and day 7 after ischemia induction of pri-miR-329, pre-miR-329 and mature miR-329-3p (B) pri-miR-494, pre-miR-494 and mature miR-494-3p (C) and pri-miR-495, pre-miR-495 and mature miR-495 (D).

Figure 3. Identification of proteins binding pre-miR-329 and pre-miR-495. (A) Schematic representation of RNA pull down combined with SILAC mass spectrometry (B) Proteins showing increased/decreased binding to pre-miR-329, pre-miR-495 or both. (C) Western blot validation of HADHB and CIRBP binding to pre-miR-329 and pre-miR-495 under conditions of normal serum and serum starvation. DHX9 is used as a binding control. (D-E) Quantification of western blot showing HADHB (D) and CIRBP (E) binding to pre-miR-329 and pre-miR-495 under conditions of normal serum and serum starvation (relative to input) *$p<0.05$, n=3.

Figure 4. Expression of CIRBP and HADHB *in vivo*. (A-B) Immunohistochemical staining of the murine adductor muscle after ischemia induction revealed expression of both CIRBP (A) and HADHB (B) in these tissues, predominantly in the cytoplasm of cells. (C-D) Microarray analysis of mRNA expression of CIRBP (C) and HADHB (D) mRNA in the adductor muscle of mice at several time points after induction of ischemia (4 mice per timepoint). (E) Western blot showing HADHB levels in murine adductor muscle tissue at day 0, day 1 and day 3 after hindlimb ligation. At each time point samples from right *(R)* unligated paws and left *(L)* ligated paws are presented next to each other. Tubulin is used as a loading control. (F) Quantification of western blot, HADHB signal was normalized against tubulin and the relative change between ligated and unligated is presented. Each bar represents a biological triplicate and technical duplicate.

Figure 5. RNA binding protein immunoprecipitation with HADHB and CIRBP antibodies. Pri-miR-329, pre-miR-329 and mature miR-329 expression levels were measured

in 3T3 cell lysates after immunoprecipitation with HADHB (top) and CIRBP (bottom) antibodies and non-specific IgG antibody. Bars represent technical tripliclates.

Figure 6. Generation of NIH-3T3 HADHB KO cell lines by CRISPR/Cas9. (A) Western Blot analysis of HADHB protein levels in two HADHB KO clones (AQ and Z) compared to decreasing amounts of total protein extract from WT NIH-3T3 cells. (B) Alignment of region surrounding CRISPR-Cas9 target sequence from genomic DNA of clones AQ and Z. Levels of mature (C) or precursor (D) miR-329 and miR-495 as well as control miR-423 in WT and HADHB KO cell lines quantified by qRT-PCR and normalized to miR-16. For pre-miRs, n=3, for mature miRs, n=9.

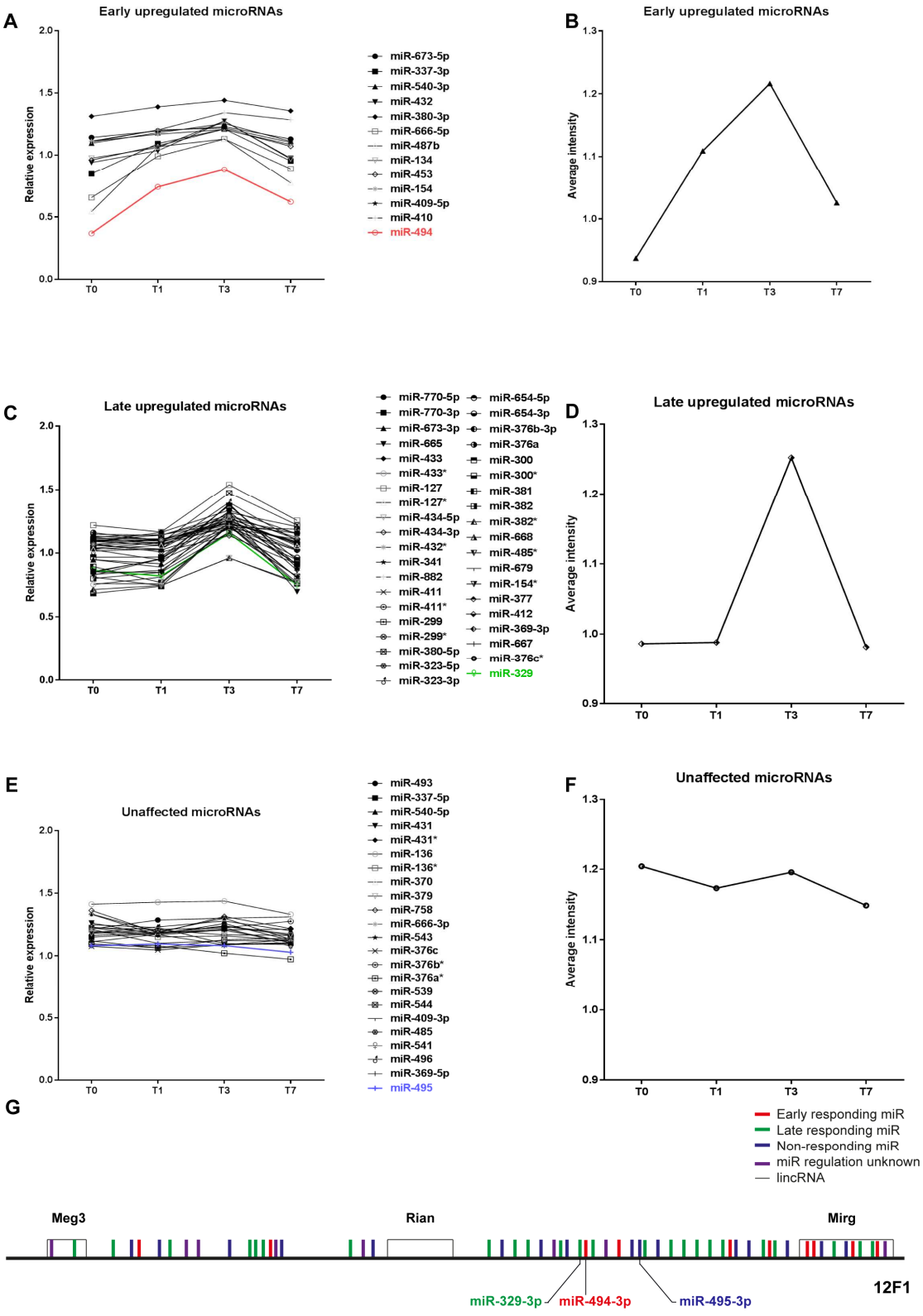
A
Early upregulated microRNAs
Relative expression
T0
T1
T3
T7
miR-673-5p
miR-337-3p
miR-540-3p
miR-432
miR-380-3p
miR-666-5p
miR-487b
miR-134
miR-453
miR-154
miR-409-5p
miR-410
miR-494
B
Early upregulated microRNAs
Average intensity
C
Late upregulated microRNAs
miR-770-5p
miR-770-3p
miR-673-3p
miR-665
miR-433
miR-433*
miR-127
miR-127*
miR-434-5p
miR-434-3p
miR-432*
miR-341
miR-882
miR-411
miR-411*
miR-299
miR-299*
miR-380-5p
miR-323-5p
miR-323-3p
miR-654-5p
miR-654-3p
miR-376b-3p
miR-376a
miR-300
miR-300*
miR-381
miR-382
miR-382*
miR-668
miR-485*
miR-679
miR-154*
miR-377
miR-412
miR-369-3p
miR-667
miR-376c*
miR-329
D
Late upregulated microRNAs
E
Unaffected microRNAs
miR-493
miR-337-5p
miR-540-5p
miR-431
miR-431*
miR-136
miR-136*
miR-370
miR-379
miR-758
miR-666-3p
miR-543
miR-376c
miR-376b*
miR-376a*
miR-539
miR-544
miR-409-3p
miR-485
miR-541
miR-496
miR-369-5p
miR-495
F
Unaffected microRNAs
G
Early responding miR
Late responding miR
Non-responding miR
miR regulation unknown
lincRNA
Meg3
Rian
Mirg
12F1
miR-329-3p
miR-494-3p
miR-495-3p

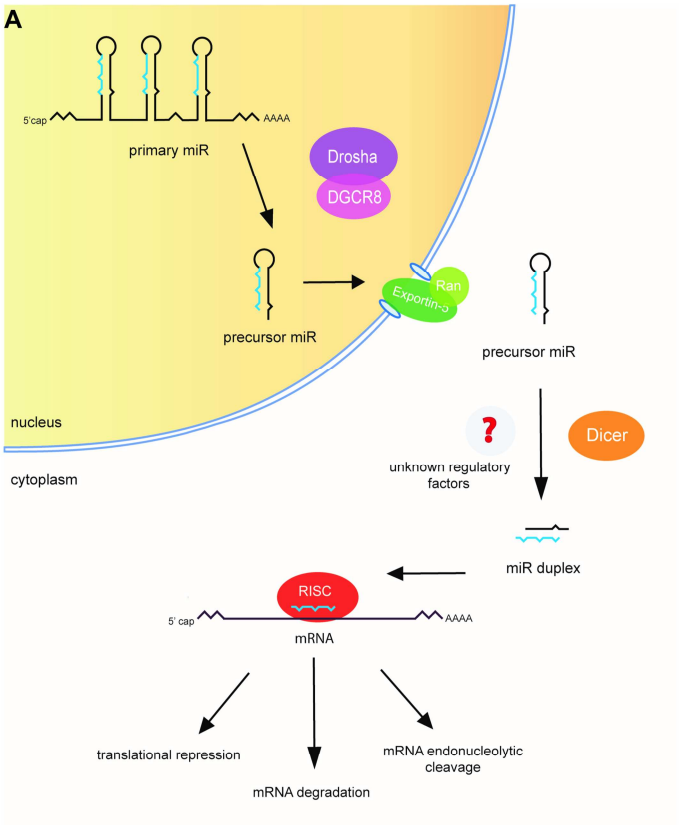

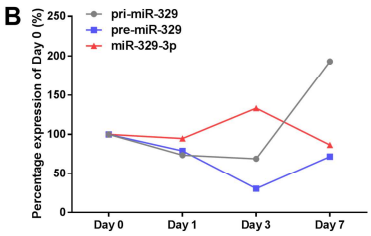

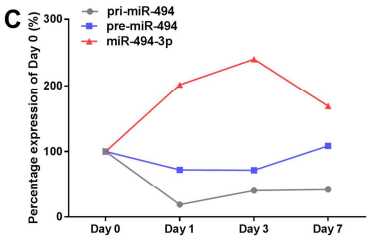

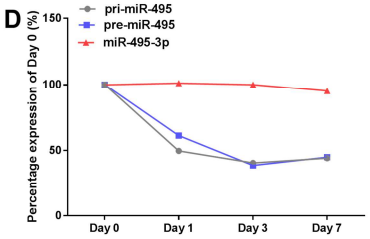

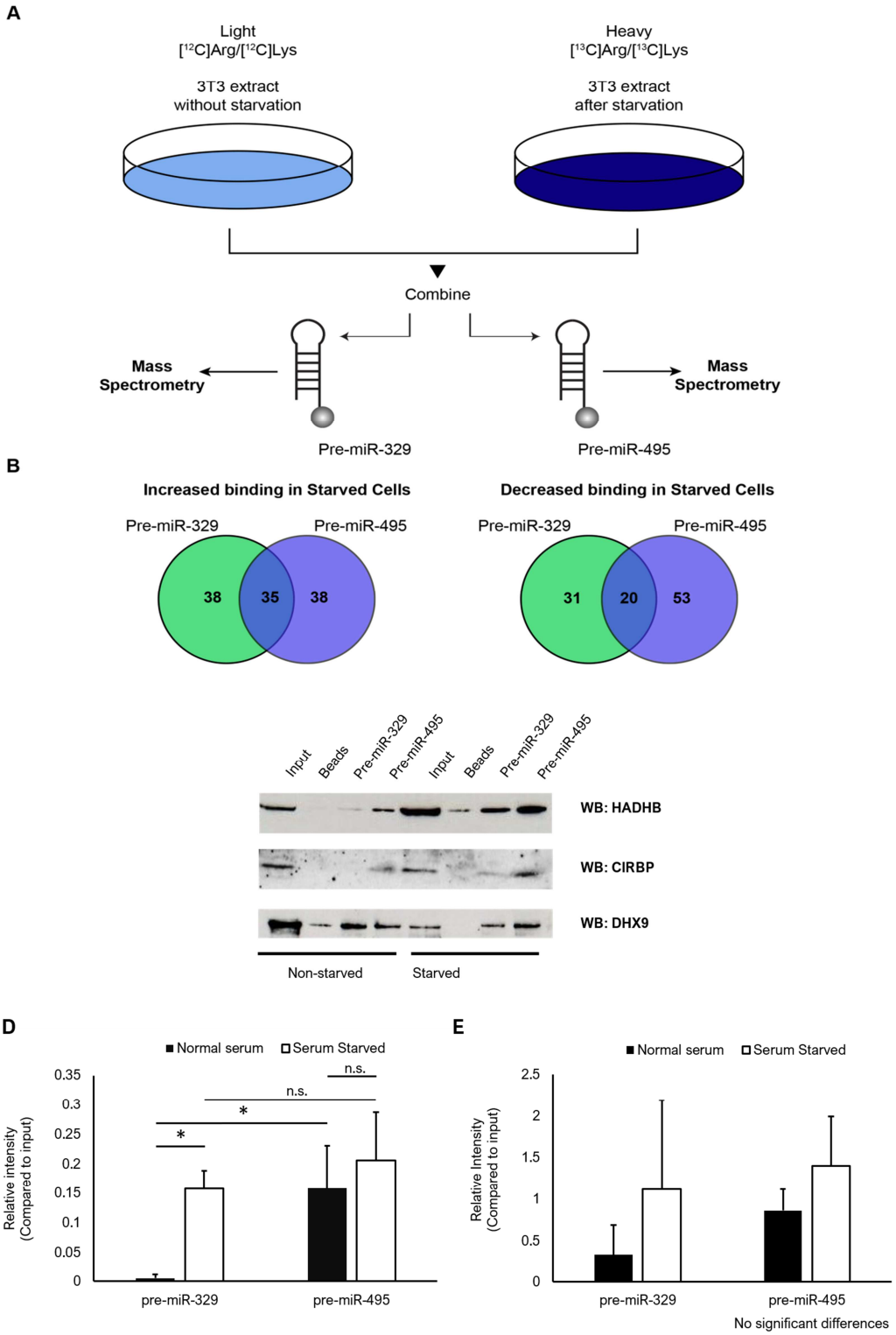
A
Light
[12C]Arg/[12C]Lys
3T3 extract
without starvation
Heavy
[13C]Arg/[13C]Lys
3T3 extract
after starvation
Combine
Mass
Spectrometry
Mass
Spectrometry
Pre-miR-329
Pre-miR-495
B
Increased binding in Starved Cells
Decreased binding in Starved Cells
Pre-miR-329
Pre-miR-495
38
35
38
31
20
53
Input
Beads
Pre-miR-329
Pre-miR-495
WB: HADHB
WB: CIRBP
WB: DHX9
Non-starved
Starved
D
Normal serum
Serum Starved
Relative intensity
(Compared to input)
n.s.
n.s.
*
*
pre-miR-329
pre-miR-495
E
Normal serum
Serum Starved
Relative Intensity
(Compared to input)
pre-miR-329
pre-miR-495
No significant differences

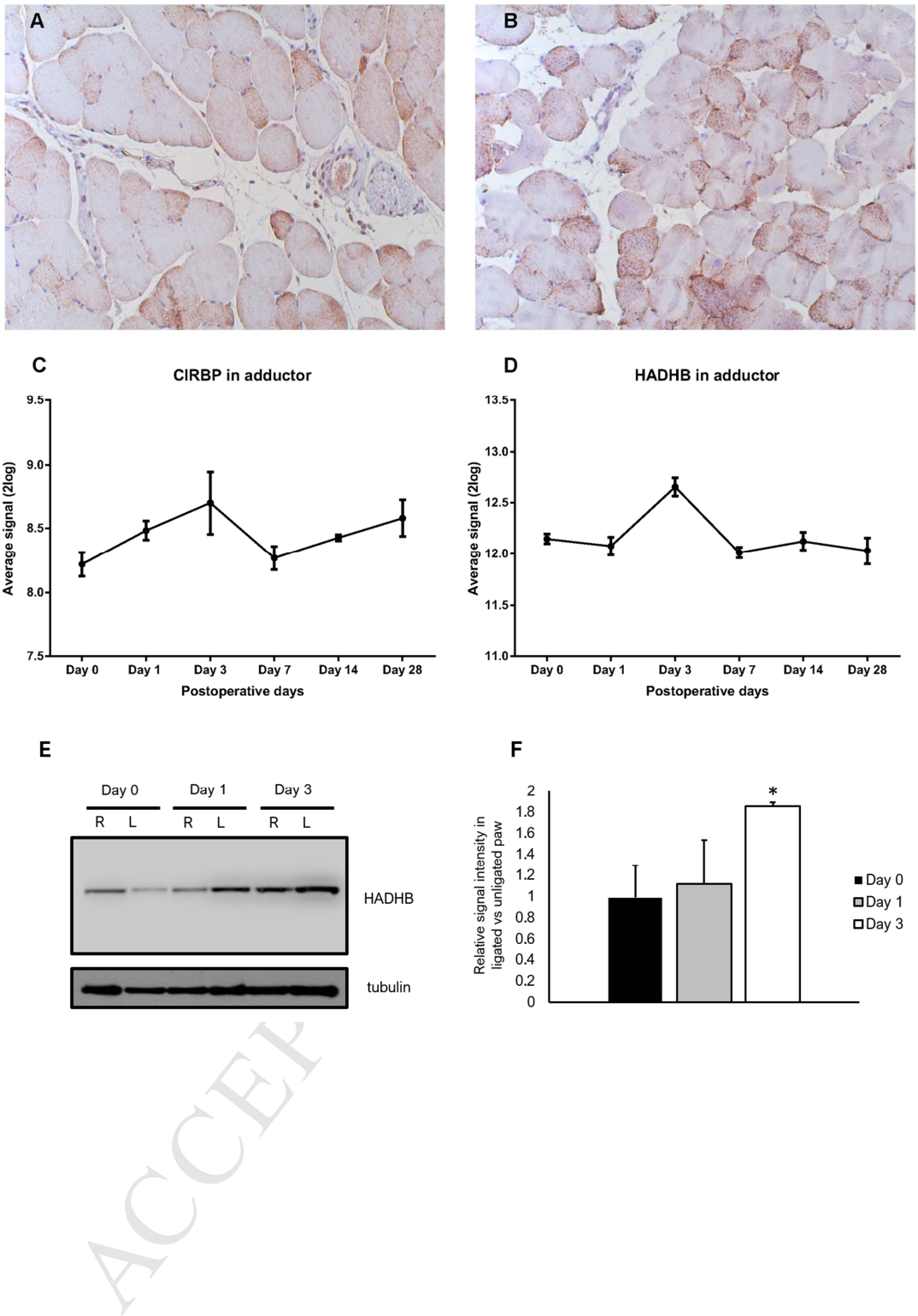
A
B
C
CIRBP in adductor
Average signal (2log)
9.5
9.0
8.5
8.0
7.5
Day 0
Day 1
Day 3
Day 7
Day 14
Day 28
Postoperative days
D
HADHB in adductor
Average signal (2log)
13.5
13.0
12.5
12.0
11.5
11.0
Day 0
Day 1
Day 3
Day 7
Day 14
Day 28
Postoperative days
E
Day 0
Day 1
Day 3
R L R L R L
HADHB
tubulin
F
Relative signal intensity in ligated vs uniligated paw
2
1.8
1.6
1.4
1.2
1
0.8
0.6
0.4
0.2
0
*
Day 0
Day 1
Day 3

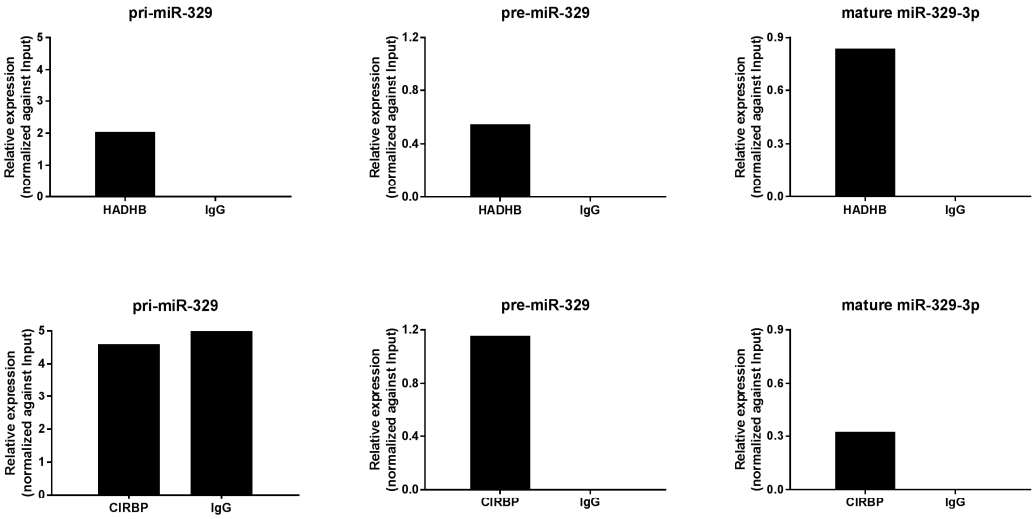

A

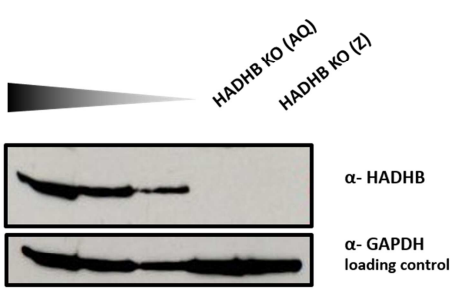

B

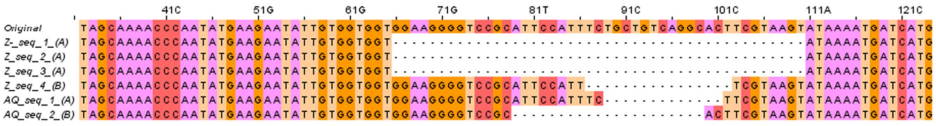

C

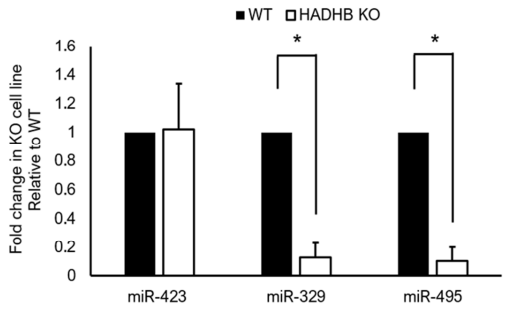

D